

A Dissertation on
Fission dynamics of ^{268}Sg formed in $^{30}\text{Si}+^{238}\text{U}$ reaction
around the Coulomb barrier.

Submitted in partial fulfillment for the requirement of
the award of the degree of
Master of Science
in
PHYSICS

Under
the supervision of
Dr. Manoj K. Sharma
(Associate Professor)

Submitted by
Rimi Singh
Roll no: - 301004014



School of Physics and Materials Science
Thapar University
Patiala (Punjab) – 147004
July 2012

Dedicated To My Loving
Father
BALWINDER SINGH
BABA

CERTIFICATE

I hereby certify that the work which has been presented in this thesis entitled, "**Fission dynamics of ^{268}Sg formed in $^{30}\text{Si}+^{238}\text{U}$ reaction around the Coulomb barrier**" submitted in partial fulfillment of the requirements for the award of degree of **Master of Science in Physics at Thapar University, Patiala**, is an authentic record of my own work carried out under the supervision of **Dr. Manoj K. Sharma, Associate Professor, SPMS** and refers other researcher's work which are duly listed in reference section.

The matter embodied in this thesis has not been submitted for the award of any other degree of this or any other university.

Date: 13 July 2012

Rishi Singh
(Rishi Singh)

This is to certify that the above statement made by the candidate is correct and true to best of my knowledge.

Manoj

Dr. Manoj Kumar Sharma
Associate Professor
SPMS, Thapar University
Patiala

Countersigned by:

Kulvir Singh

Dr. Kulvir Singh
Professor & Head
SPMS, Thapar University
Patiala

S.K. Mohapatra

Dr. S.K. Mohapatra
Dean of Academic Affairs
Thapar University,
Patiala

Acknowledgement

With deep sense of gratitude, I would like to express my sincere thanks to all those who gave me the possibility to complete thesis dissertation work.

First of all, I want to thanks my supervisor, **Dr. Manoj Kumar Sharma**, Associate Professor, Thapar University, Patiala. He is always willing to listen, discuss and advice throughout the work. The encouragement and guidance from him is always appreciated. Thanks are also due to Mrs. Manpreet Kaur, research scholar for useful discussions and helpful feedbacks. I am sure that the knowledge gained through my association with her shall go a long way in helping me to achieve the success in my life.

I would like to express my sincere regards to **Dr. Kulvir Singh**, Associate Professor and Head, School of Physics and Materials Science for support and providing facilities.

I would like to thank My Father **Sh. Balwinder Singh Batta**, My Mother and My loving brothers Gagandeep, Bawa, Gurinder, Dalbir. This work would not have been possible without them. And I want to thanks my friends Aman and Gurpreet who have been a constant source of support.

Ms. Rimi Singh

(301004014)

ABSTRACT

The aim of present work is to study the possible decay modes of the nuclear system at energies around the Coulomb barrier. In the process, issues related to fusion-fission fragments, deformation and orientation effects, etc., are investigated. The tough challenges in nuclear perspective can be met only by developing and establishing clear understanding of related phenomena on the theoretical front, which could be utilized to plan and implement the predictions through experiments. A number of factors and properties influence the fusion-fission process and hence need to be handled with proper care in order to make meaningful predictions. The Dynamical Cluster Decay Model (DCM) is used to investigate the Fusion- fission of ^{268}Sg formed in $^{30}\text{Si}+^{238}\text{U}$ reaction around the Coulomb barrier. The calculations have been done in the framework of Dynamical Cluster decay Model (DCM). We have calculated the fission cross-sections in reference to available experimental data. The decay has been analysed for the quadrupole (β_2) deformed fragmentation. The calculated cross-sections compare nicely with the available experimental data within one parameter fitting, the neck length ΔR .

CHAPTER: 1	PAGE NUMBER
1.1 Introduction.....	9
1.2 Factor that may effect the decay path paths of nuclear system.....	11
1.3 Quasi fission in super-heavy mass region.....	12
1.4 Heavy ion collisions in the nucleonic regime.....	12
1.5 Heavy ion nuclear reaction.....	13
1.6 Fusion reaction.....	15
1.7 Hot fusion reaction.....	17
1.8 Deformed nuclei.....	17
1.9 Effect of deformed nuclei.....	17
Reference.....	20
 CHAPTER: 2	
Methodology.....	22
2.1 The Fragmentation potential $V(\eta)$	25
2.1.1 The Proximity Potential for deformed, oriented and coplanar nuclei.....	25
2.1.2 The Coulomb potential.....	25
2.1.3 Angular momentum dependent potential.....	26
2.2 Quantum Mechanical Fragmentation Theory.....	26
2.3 Preformation Probability (P_0).....	27

2.4 Penetration Probability (P).....28

Reference.....29

CHAPTER: 3

3.1 Results and discussions.....30

Summary.....41

References.....42

LIST OF FIGURES

Figure 1.1 Diagram showing evaporation, fission and quasi-fission process.

Figure 1.2 A nuclear (Z-N) landscape, the chart of bound as well as unbound nuclear systems.

Figure 1.3 Binding energy per nucleon as a function of mass number.

Figure 1.4 Potential Barrier vs. deformation.

Figure 2.1 Scattering Plot for $^{30}\text{Si} + ^{238}\text{U} \rightarrow ^{268}\text{Sg} \rightarrow A_1 + A_2$ reaction

Figure 3.1(a) shows the fragmentation potential as the function of fragment mass considering β_2 deformed fragmentation path at lowest energy $E_{cm} = 124.90 \text{ MeV}$.

Figure 3.1(b) shows the fragmentation potential as the function of fragment mass considering β_2 deformed fragmentation path energy at highest $E_{cm} = 169.1 \text{ MeV}$.

Figure 3.2(a) shows the preformation probability as the function of fragment mass for ^{268}Sg compound system at lowest energy $E_{cm} = 124.90 \text{ MeV}$.

Figure 3.2(b) shows the preformation probability as the function of fragment mass for ^{268}Sg compound system at lowest energy $E_{cm} = 124.90 \text{ MeV}$.

Figure 3.3 Preformation probability, Penetrability and cross-section as the function of mass fragments A_2 at $E_{cm} = 124.90 \text{ MeV}$.

Figure 3.4 (a) penetrability as a function of mass fragments A_2 at $E_{cm} = 124.90 \text{ MeV}$.

Figure 3.4 (b) penetrability as a function of mass fragments A_2 at $E_{cm} = 169.1 \text{ MeV}$.

Figure 3.5 Decay of barrier height as a function of mass fragments A_2 at lowest energy $E_{cm} = 124.90 \text{ MeV}$.

Figure 3.6 DCM based cross-section compared with experiment.

Figure 3.7 Neck length parameter as a function of E_{cm} .

Figure 3.8 ΔV_b as a function of E_{cm} .

Chapter 1:

1.1 Introduction:

One of the major aspects of today's nuclear physics research is to look for a right kind of target and projectile combinations in order to synthesize a heavy and super heavy nuclear system. Proper choice of target projectile combination is of extreme important to maximize the cross section for production of super heavy nuclei in the laboratory [1]. Formation of a super heavy nuclear system requires fusion of two heavy nuclei. In such nuclear reactions the nucleons of the projectile must interact with the nucleons of the target. Therefore the energy must be high enough to overcome the natural electromagnetic repulsion between the protons of colliding nuclei. This energy "barrier" is called the Coulomb barrier. Since the probability of decay of a compound nucleus increases with excitation energy, it is desirable that compound nucleus is produced at moderate excitation energy, i.e.; near the Coulomb barrier energy where fusion cross section is not very low.

When a target nucleus is hit by a projectile nucleus near the Coulomb barrier energy, the contributions in reaction cross-sections comes mainly from the three processes:

(i) *Fusion evaporation residue cross-section:* when projectile hits a target, the resulting a compound nucleus (CN) is relatively stable but excited with fairly large angular momentum. The compound nucleus (CN) state is formed by overcoming the Coulomb repulsion and consequently an attractive potential pocket is formed due to strong nuclear forces. This compound nucleus now loses some of this excess energy in the form of α -particle, neutron, proton and γ -rays. Normally if, available energy is sufficiently large then α -particle is emitted otherwise smaller particle like neutron, protons etc. are emitted. As the system is in excited state so the (ground-state) stable condition is achieved via emission of γ -rays. Normally ER are very prominent in case of lighter nuclei and this process is superseded by fission when relatively higher mass

nuclear system are taken into consideration. Alternatively, in some cases the non compound nucleus (NCN) components start competing into fission and ER. Such NCN compound may comprise of quasi fission (qf), incomplete fusion (ICF) etc.

(ii) *fusion-fission cross-section*: In fusion-fission process the compound nucleus is normally in an excited state and excitation energy depends on the energy of fusion reaction. It loses this excitation energy in various ways. For the heavy nuclear systems the most probable decay mode of the compound nucleus is fission, due to its instability against centrifugal repulsion. However for light compound systems with $A < 80$ there is a competition between decay modes (fission verses fusion evaporation residue).

(iii) *Quasi-fission or deep inelastic collision cross-section*: The third main type of reaction is the deep-inelastic reaction. Deep inelastic collisions of nuclei are very energetic collisions. Such reactions involve heavier ions and generally take place at intermediate impact parameter. For large impact parameter they go over into the direct or quasi-elastic reaction and for small impact parameter into fusion. The important difference between ER, fission and deep inelastic reaction is that the compound nucleus formations take place in first two whereas third one is non-compound nucleus reaction. With this non-compound nucleus reaction if the emitted products are identical with the formation partners, the reaction is called as quasi-fission reaction or quasi-fission process. It is the phenomenon in which target and projectile nuclei collides with each other and forms a di-nuclear system (DNS) which decays into the product nuclei which is identical to the target and projectile is called quasi-fission. Or quasi fission means re-separation of di-nuclear molecular complex before the compound nucleus formation.

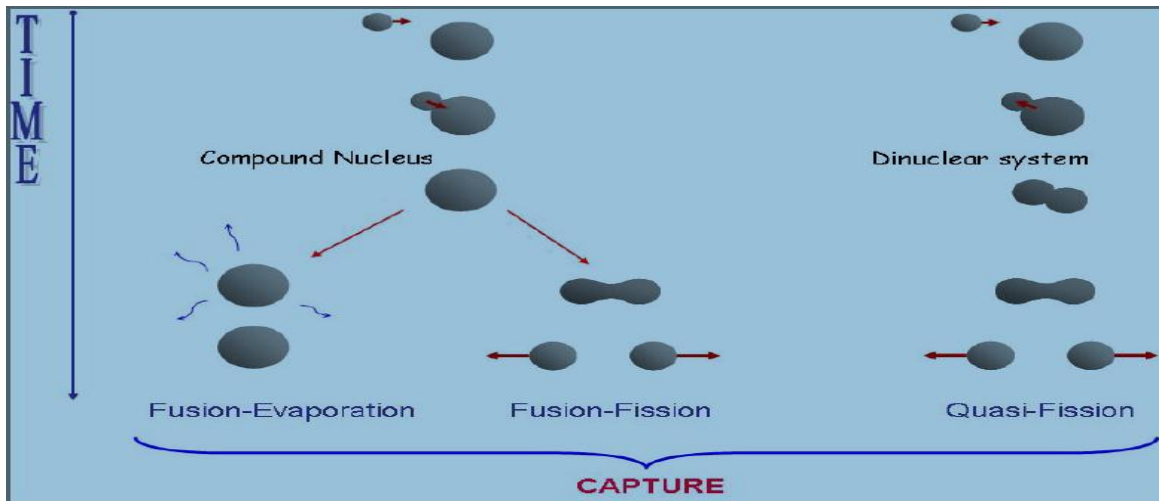


Figure: 1.1 Diagram showing evaporation, fission and quasi-fission process.

It may be mentioned here that quasi-fission is different from the fast-fission [2] or pre-equilibrium fission reactions. The fast fission occurs for a composite system when the angular momentum dependent fission barrier drops below the nuclear temperature and becomes extremely small. In the case of pre-equilibrium (PEQ) fission, the composite nucleus breaks before complete equilibration in shape or K degree (K being the projection of total angular momentum on the symmetry axis of the fissioning nucleus) of freedom. The major difference between PEQ fission and quasi-fission is that, while PEQ fission follows the formation of a compact mononuclear system or ER, quasi-fission does not form such composite state.

1.2 Factors that may effect the decay paths of a nuclear system:

- Excitation energy.
- Angular momentum.
- Entrance channel mass asymmetry.
- Nuclear deformation and orientation.

1.3 Quasi fission in super-heavy mass region:

Evidence of formation of long-lived isotopes of elements with $z = 113, 114, 116$ and 118 [3-6] have recently energized experimental efforts. Such experiments are extremely challenging as the formation of heavy/super-heavy evaporation residues (ER) is heavily suppressed not only by equilibrium fission, but also by a non-equilibrium process called quasi-fission [7-10]. The development of theoretical models to predict cross-sections for nuclei located at the extreme end of heavy elements is important for the proper understanding of nuclear dynamics and related features. A large amount of data is made available on competing NCN process like quasi fission, deep in elastic collision, ICF etc and consequently the existing theoretical models are improved to handle this complex decay mechanism. In majority of models, the reaction is supposed to proceed via three steps: (1) penetration of the Coulomb barrier between two colliding nuclei, (2) formation of a compound barrier, and (3) survival of the excited compound nucleus against fission (fusion – fission) to produce evaporation residue (ER).

In a reaction using a heavy target and projectile, which is the case for the production of the heaviest element, quasi fission competes against fusion fission process.

1.4 Heavy ion collisions in the nucleonic regime:

The last decades have seen an accumulation of an impressive corpus of nuclear properties close to equilibrium. What picture does the heavy-ion collisions present scenario display? The answer is that the study of heavy ion-collisions in the nucleonic regime is two fold. Firstly, there is an interest in understanding the time evolution of the reaction starting from a highly-out-of-equilibrium situation (two cold colliding nuclei) towards a possible thermalized system by means of dissipation and secondly, reaction products are in extreme states in the sense that they can be highly exotic or hot. Exotic nuclei have unusual neutron/proton ratio or a very large number of

neutrons (super heavy elements). Hot nuclei have excitation energies close or even higher than their total binding energies. Studies of nuclei at finite temperatures are incomplete without an explicit account of the dynamics involved.

1.5 Heavy ion nuclear reactions:

Since the first experimental demonstration of nuclear reaction process by Rutherford in 1919, experimental techniques in the field of nuclear physics have improved immensely. Formerly, in the study of nuclear reactions the projectiles used were basically the alpha particles from natural radioactive substances. Also, the discovery of neutron in 1932 caused an impetus in the nuclear reaction experiments. Low energy neutrons can easily penetrate Coulomb barrier and cause nuclear reactions. Later on, the advent of highly advanced particle accelerators techniques has made possible high energy beams of not only protons, deuterons and alpha particles but also heavy ions, to produce nuclear reactions. Highly efficient and precise detector technology, to observe nuclear phenomena, is available. Fast computational methods further aided in precise and accurate measurements of cross sections and angular distribution of the disintegration products in the experiments.

In the last few decades, nuclear reactions have played a significant role in the discovery of many nuclei away from the valley of stability. By adding neutrons or protons to a nucleus, the nucleus does not accept any more nucleons after a certain number. So at this limit the separation energy of the proton or the neutron has reached zero. These limitations are called proton and neutron drip lines which are placed on the sides of the valley of stability. In the valley of stability, the heaviest stable nucleus is with ($N = 126$, $Z = 82$) which is a doubly magic nucleus. The next doubly magic stable nucleus heavier than Pb is predicted to be at ($Z = 114$, $N = 184$) within the sea of instability. This island of stability is so called the region of super heavy elements. That

means there exists a number of nuclei around the stable magic nucleus with ($Z = 114$, $N = 184$) which are relatively stable nuclei in the sea of instability, the so-called island of stability of super heavy elements and hence 114 is called the stepping stone for super heavy elements in reference to island of stability.

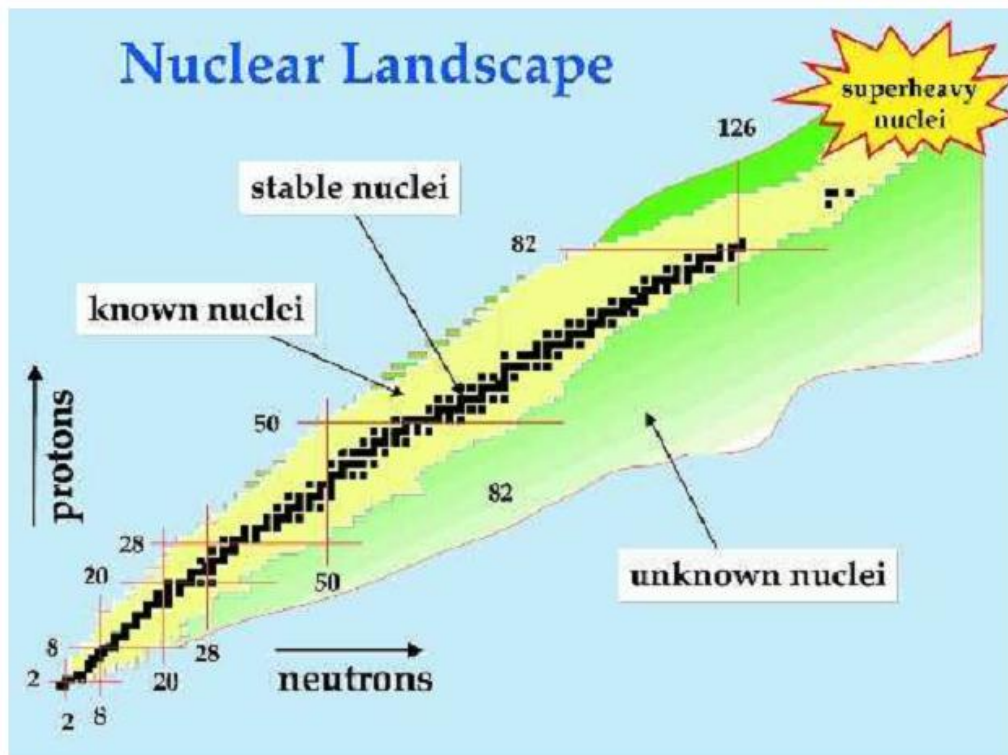


Figure 1.2: A nuclear (Z-N) landscape, the chart of bound as well as unbound nuclear systems ([http://www.anl.gov/.../070608 nuclear landscape-200.jpg](http://www.anl.gov/.../070608_nuclear_landscape-200.jpg)).

The valley of stability (Figure 1.2) comprises bound/ stable nuclear systems in the Z-N landscape, popularly known as “nuclear landscape”, a chart plotted as a function of proton number Z and neutron number N. It is worth notice that that about 8 thousand combinations of protons and neutrons are possibly involved in the nuclear landscape.

A nuclear reaction is described by identifying incident particle/nucleus with specific associated incident energy, target nucleus, and reaction products. The nuclear reactions play an

important role in the production of new elements, their further studies and application, etc. For successful formation of heavy nuclei, deep understanding of fusion-fission process of the compound nucleus formed in heavy ion reaction is essential. The study of heavy ion reaction induced reaction has been directed toward this aim since the dream of super heavy element was seen in the late sixties of last century.

1.6 Fusion reaction:

Nuclear fusion is the process in which multi atomic nuclei join together to form a heavier nucleus. It is followed by the release or absorption of energy. From Figure 1.3, one can see that iron and nickel nuclei are the most stable nuclei and they have the largest binding energy per nucleon. Therefore, a fusion reaction of nuclei lighter than iron and nickel release energy and reactions of nuclei heavier than iron and nickel absorbs energy. A substantial energy barrier, due to mutual repulsion between the two nuclei, opposes the fusion reaction. This barrier consists of the Coulomb and the nuclear potentials. However, the long range Coulomb repulsion between the nuclei is offset by the strong, but the short range, attractive nuclear force. Only problem is to bring the nuclei sufficiently close so that the Coulomb barrier can be crossed over, say, via tunneling. Hence, the two nuclei are required to collide with sufficient kinetic energy to overcome their mutual electrostatic repulsion (or fusion threshold barrier) and the subsequently to bring into the effect of strong but short range attractive nuclear force. In other words, the simplest picture of fusion is obtain by studying the quantum tunneling through a one dimension barrier formed by the long range Coulomb potential, the centrifugal potential and the short range nuclear potential. It means that the knowledge of interaction potential, forming potential, between two nuclei is extremely important in order to have a systematic study of nuclear reaction [11-15].

Nuclear fusion occurs naturally in stars and also has been made artificially but it is not completely controlled.

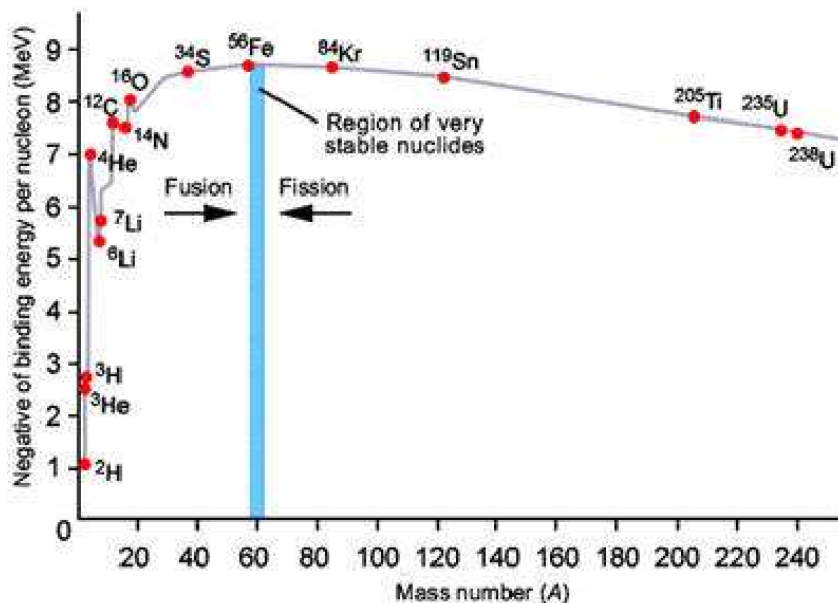


Figure 1.3: Binding energy per nucleon as a function of mass number.

It is well known that heavy and super heavy nuclei are synthesized in heavy ion fusion reactions. In order to find the mechanism of producing compound nuclei from these reactions, there are two different approaches known as cold fusion and hot fusion reactions. These methods depend on parameter which is the excitation energy of the compound nucleus that gives a maximum result of the reaction [16]. In the cold fusion reactions, lead and bismuth targets are used [17]. The super heavy nuclei (SHN) synthesized in the cold fusion reaction produce nuclei with relatively small number of neutrons. But the hot fusion reactions, on the other hand, use actinide nuclei as targets have relatively large number of neutron in the vicinity of $N=184$. With this type of reactions, production of elements with $Z = 114, 115, 116, 117,$ and 118 are reported by the Flerov Laboratory of Nuclear Reactions (FLNR) [18]. These nuclei as well as those produced as

descendants in the α -decay chain have relatively larger number of neutrons. Recently, other laboratories than FLNR also performed experiments of hot fusion reactions and obtained results that are consistent with the data by FLNR [19–22]. At present, attempts to produce elements 119 and 120 are made or planned in several facilities using actinide targets. In order to produce new nuclei or elements not discovered so far, an accurate prediction of the production cross sections is an important issue in the SHN research.

1.7 Hot fusion:

The hot fusion reactions to produce super heavy elements, always involve a heavy target in the region of actinide nuclei with light projectile nuclei. The heavy target includes many protons which give rise to the Coulomb barrier. This implies that the projectile must have a high energy to overcome the Coulomb barrier. If the reaction partners considered are deformed then there is a substantial decrease in the barrier height and hence the penetration becomes easier.

1.8 Deformed nuclei:

Not all nuclei have the spherical shape with closed shells. In the heavy and super heavy mass region, nuclei have non spherical charge distributions even in their ground states. These deformed shapes govern the electric quadrupole moment. These nuclei are away or far away from closed shell with deformed shapes. These deformations include additional modes of nuclei to be in excited state with a possible change in of their electric quadrupole moment.

1.9 Effects of deformed nuclei:

The depth and the width of the capture well in the nucleus-nucleus interaction potential, as well as the barrier height are known to play a dominant role in the dynamics of a compound nucleus formed in heavy ion reactions. This feature is associated with the necessity to overcome the

barrier that exists between two separated nuclei and with a formation of a scission neck between contacting nuclei in the capture well, as well as with the following evolution of shape of the nuclear system. Therefore, it is very important to study the influence of deformation and orientation on the nucleus-nucleus interaction potential. It has been observed that when we opt for a deformed target/ projectile combination for the synthesis of heavy/ super heavy nuclei the fusion probability in general gets increased as the barrier gets modified with inclusion of deformation & orientation effects.

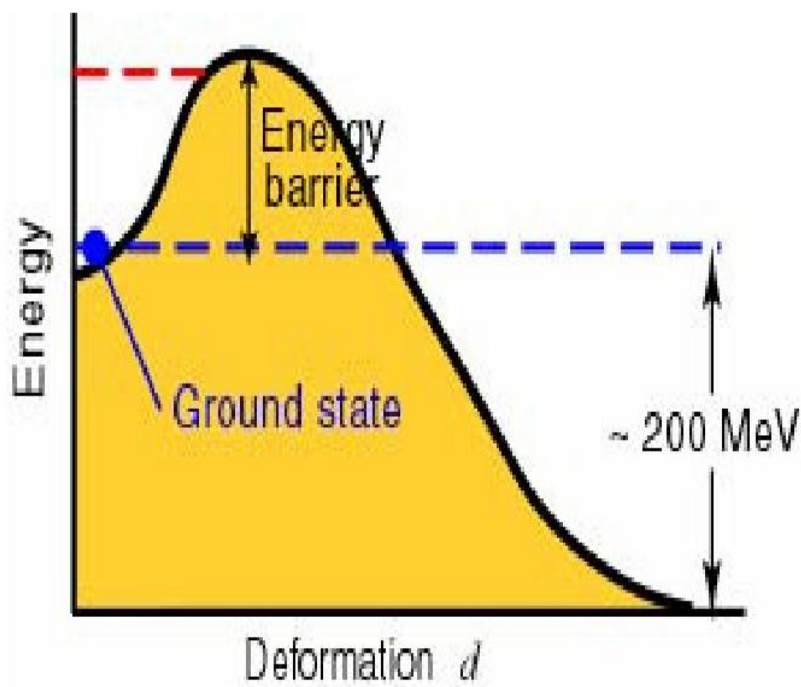


Figure 1.4 Potential Barrier vs. deformation.

The apparent reason for this enhancement in fusion probability is that the inclusion of deformation and orientation effects of the colliding nuclei leads to lowering of its barrier height to provide easier path for compound nucleus formation. The collisions between deformed as well

as oriented nuclei have been studied extensively using DCM to establish the effect of deformation and orientation on fusion reactions [11-15].

In the present work, we have studied the decay of ^{268}Sg formed in $^{30}\text{Si}+^{238}\text{U}$ reaction. ^{268}Sg is a super heavy nuclear system having $Z=106$. Here we have concentrated only on the fusion-fission dynamics of ^{268}Sg . For this purpose, we have made calculation using the **dynamical cluster model** (DCM). It is relevant to mention here that DCM has been used quite extensively to study the heavy ion reactions in light, intermediate, heavy and super heavy mass region during last one decade.

Reference:

- [1] Yu. Ts. Oganessian *et al.*, Phys. Rev. C 74, 044602 (2006).
- [2] B.B. Back *et al.*, Phys. Rev. C. **32**, 195 (1985), Phys. Rev. Lett. **46**, 1068 (1981).
- [3] K.Morita *et al.*, J. Phys. Soc. Jpn. 73, 2593 (2004).
- [4] Yu. Ts. Oganessian *et al.*, Nature (London) 400, 242(1999).
- [5] Yu.Ts. Oganessian *et al.*, Phys. Rev. C 63, 011301(R) (2000).
- [6] Yu. Ts. Oganessian *et al.*, Phys. Rev. C 74, 044602 (2006).
- [7] W. J. Swiatecki, phys. Scr. 24, 113 (1981).
- [8] S. Bjornholm and W. J. Swiatecki, Nucl. Phys. A391, 471 (1982).
- [9] J. P. Blocki *et al.*, Nucl. Phys. A459, 145 (1986).
- [10] P. Moller and A. J. Sierk, Nature (London) 422, 485 (2003).
- [11] R. Kumar & M. K. Sharma Phys. Rev. C 85, 054612 (2012); D. Jain, R. Kumar, M. K. Sharma & R.K Gupta, Phys. Rev. C 85, 024615 (2012).
- [12] M. K. Sharma, G. Sawhney, R. K. Gupta, W. Grenier, J.Phys.G:Nucl.Part.Phys. 38 105101 (13pp) (2011); K. Sandhu, M. K. Sharma, R. K. Gupta, Phys. Rev. C 85 024604 (2012).
- [13] B. B. Singh. M. K. Sharma and R. K. Gupta, Phys. Rev. C 77 054613 (2008); M. Kaur, R. Kumar and M. K. Sharma Phys. Rev. C 85 014609 (2012); M. Kaur, M. K. Sharma Phys. Rev. C 85 054605 (2012).
- [14] R. K. Gupta, M. Balasubramaniam, R. Kumar, N. Singh, M. Manhas, and W. Greiner, J. Phys. G: Nucl. Part. Phys. C 31, 631 (2005); M. Manhas and R. K. Gupta, Phys. Rev. C 72, 024606 (2005).
- [15] R. K. Gupta, M. Manhas, G. MÄunzenberg, and W.Greiner, Phys. Rev. C 72, 014607 (2005).

- [16] Yu.Ts. Oganessian. Reactions of synthesis of heavy nuclei brief summary and outlook. *Physics of atomic nuclei*, 69:932–940, 2006.
- [17] S. Hofmann and G. Münzenberg, *Rev. Mod. Phys.* **72**, 733 (2000); S. Hofmann *et al.*, *Eur. Phys. J. A* **14**, 147 (2002).
- [18] Yu. Ts. Oganessian *et al.*, *Nature* **400**, 242 (1999); *Phys. Rev. Lett.* **83**, 3154 (1999); *Phys. Rev. C* **62**, 041604(R) (2000); **63**, 011301(R) (2000); **69**, 021601(R) (2004); **72**, 034611 (2005); **74**, 044602 (2006); **76**, 011601(R) (2007); *Phys. Rev. Lett.* **104**, 142502 (2010).
- [19] S. Hofmann *et al.*, *Eur. Phys. J. A* **31**, 251 (2007).
- [20] L. Stavsetra, K. E. Gregorich, J. Dvorak, P. A. Ellison, I. Dragojević, M. A. Garcia, and H. Nitsche, *Phys. Rev. Lett.* **103**, 132502 (2009).
- [21] P. A. Ellison *et al.*, *Phys. Rev. Lett.* **105**, 182701 (2010).
- [22] Ch.E. Düllmann *et al.*, *Phys. Rev. Lett.* **104**, 252701 (2010).

Chapter 2

Methodology:

This work deals with the study of heavy ion reaction dynamics using the Dynamical Cluster-decay Model (DCM) [1-5]. The DCM, worked out in terms of the collective coordinates of mass asymmetry $\eta = A_1 - A_2 / A_1 + A_2$ and relative separation R respectively gives the nucleon-division between the outgoing fragments, and the transfer of kinetic energy of incident channel (E_{cm}) to internal excitation (total excitation or total kinetic energy, TXE or TKE) of the outgoing channel. This energy transfer process can be calculated with the help of equation

$$E_{CN}^* = E_{c.m} + Q_{in} = IQ_{out} + TKE(T) + TXE(T) \quad (2.1)$$

The CN excitation E_{CN}^* is related to temperature T (in MeV) and is given by

$$E_{CN}^* = aT^2 - T(Mev) .$$

Where level density, $a = A/9$.

DCM defines the decay cross section, in terms of partial waves using the decoupled approximation to R and η -motions as:

$$\sigma = \frac{\pi}{k^2} \sum_{l=0}^{\ell_{max}} (2l+1) P_0 P \quad (2.2)$$

$$k = \sqrt{\frac{2\mu E_{c.m}}{\hbar^2}}$$

Where P_0 is the preformation probability refers to η -motion and P is the penetrability to the R -motion. The structure information of the CN enters the model via preformation probability P_0 .

(also known as spectroscopic factor) of the fragments given by the solution of stationary Schrödinger equation in η at the fixed $R=R_a$

$$\left\{ -\frac{\hbar^2}{2\sqrt{B_{\eta\eta}}} \frac{\partial}{\partial \eta} \frac{1}{\sqrt{B_{\eta\eta}}} \frac{\partial}{\partial \eta} + V_R(\eta, T) \right\} \psi^v(\eta) = E^v \psi^v(\eta) \quad (2.3)$$

With $v=0, 1, 2, 3, \dots$ referring to the ground state and excited state solution. R_a is the first turning point of the penetrability path shown in figure 2.1 for the different ℓ -values. The potential $V(R_a)$ acts like an effective Q-value, Q_{eff} , for the decay of the hot CN at temperature T , to two exit-channel fragments observed ($T=0$), defined by

$$Q_{\text{eff}}(T) = B(T) - [B_L(T=0) + B_H(T=0)] = \text{TKE}(T) = V(R_a(T)) \quad (2.4)$$

with B 's as the respective binding energies.

The above defined decay of a hot CN into two cold ($T=0$) fragments, via Eq (2.4), could apparently be achieved only by emitting some light particle(s) (LPs), like n , p , α , or γ -rays of energy. By defining $Q_{\text{eff}}(T)$ as in Eq. (2.4), in this model we treat the LP emission at par with the heavy fragments, called intermediate mass fragments (IMFs) emission.

Thus, in this model a non-statistical dynamical treatment is attempted for not only the emission of IMFs but also of multiple LPs, understood so-far only as the statistically evaporated particles in a CN emission. It may be reminded here that the statistical model (CN emission) interpretation of IMFs is not as good as it is for the LP production.

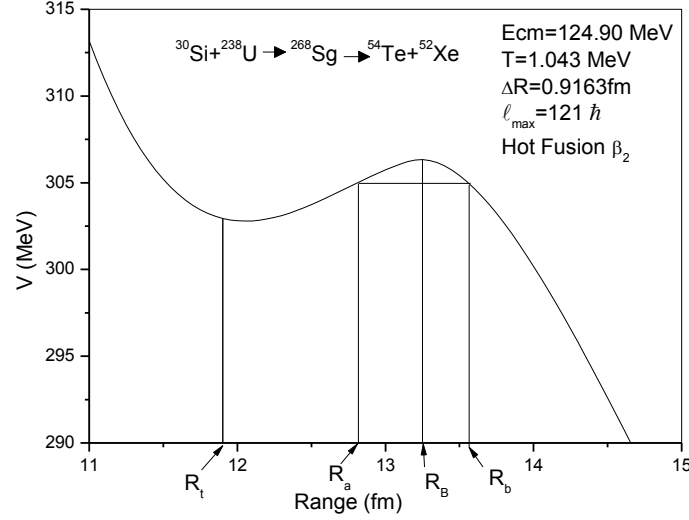


Fig 2.1 Scattering Plot for $^{30}\text{Si} + ^{238}\text{U} \rightarrow ^{268}\text{Sg} \rightarrow ^{54}\text{Te} + ^{52}\text{Xe}$ reaction.

2.1 The Fragmentation potential $V(\eta)$:

The collective potential energy or the fragmentation potential can be given by $V(\eta, R)$

$$V_R(\eta, T) = \sum_{i=1}^2 [V_{LDM}(A_i, Z_i, T)] + \sum_{i=1}^2 [\delta U_i] \exp(-T^2 / T_0^2) + V_c(R, Z_i, \beta_{\lambda i}, \theta_i, T) + V_p(R, A_i, \beta_{\lambda i}, \theta_i, T) + V_l(R, A_i, \beta_{\lambda i}, \theta_i, T) V_R(\eta, T) \quad (2.5)$$

The fragmentation potential $V(\eta)$, appearing in equation (2.3) is calculated at a fixed distance $R = R_1 + R_2 + \Delta R$ for consideration of deformed and oriented reaction product. Here $\lambda=2, 3, 4, \dots$ and α_i is an angle that the radius vector R_i of the colliding nuclei makes with the symmetry axis.

2.1.1 The proximity potential for deformed, oriented and coplanar nuclei:

When two surfaces approach each other within a small distance of less than $\sim 2\text{fm}$, comparable with the surface thickness of interacting nuclei, or when a nucleus is at the verge of dividing into two fragments, then the two surfaces actually face each other across a small gap or crevice. In

both cases, the surface energy term alone could not give rise to the strong attraction that is observed when the two surfaces are brought in close proximity. Such additional attractive forces are called proximity forces and the additional potential due to these forces is called the nuclear proximity potential.

The proximity potential is given as

$$V_P(s_0) = 4\pi \bar{R} \gamma b \Phi(s_0). \quad (2.6)$$

$\Phi(s_0)$ is the universal function, independent of the shapes of nuclei or the geometry of nuclear system, but depends on the minimum separation distance

$$\Phi(s_0) = -\frac{1}{2}(s_0 - 2.54)^2 - 0.0852(s_0 - 2.54)^3, \text{ and, } \Phi(s_0) = -3.437 \exp\left(\frac{-s_0}{0.75}\right) \quad (2.7)$$

respectively, for $s_0 \leq 1.2511$ and $s_0 \geq 1.2511$. Here, s_0 is defined in units of b , i.e. s_0 is s_0/b .

2.1.2 The Coulomb potential:

Coulomb potential is the potential which describes the force of repulsion between two interacting nuclei due to their charges, acts along the line joining the two nuclei. The Coulomb potential for two interacting nuclei is given by:

$$V_c(Z_i, \beta_{\lambda i}, \theta_i, T) = \frac{Z_1 Z_2 e^2}{R(T)} + 3Z_1 Z_2 e^2 \sum_{i, \lambda=1,2} \frac{R_i^\lambda(\alpha_i, T)}{(2\lambda+1)R(T)^{\lambda+1}} Y_\lambda^{(0)}(\Theta_i) \left[\beta_{\lambda i} + \beta_{\lambda i}^2 \gamma_\lambda^{(0)}(\Theta_i) \right] \quad (2.8)$$

With $Y_\lambda^{(0)}(\Theta_i)$ is the spherical harmonic function.

2.1.3 Angular momentum dependent potential:

$$V_l = \frac{\hbar^2 \ell(\ell+1)}{2I} \quad (2.9)$$

Here, I is moment of inertia and l is angular momentum.

2.2 Quantum Mechanical Fragmentation Theory:

The QMFT [6-8] is a unified description of two body channels in both fusion and fission processes. Here the quantum mechanical concept of probability is utilized to investigate the role of shell effects in the fusion, fission. In QMFT, nuclear dynamics is explained by the mass parameters defining the kinetic energy of the system while the static properties of nuclear system are determined by the potential energy surfaces. The QMFT is worked out in terms of the following collective coordinates:

(i) Relative separation coordinate R between the two nuclei or, in general, two fragments (or, equivalently, the length parameter $\lambda=L/2R_0$, with L as the length of the nucleus and R_0 as the radius of an equivalent spherical nucleus).

(ii) Mass and charge fragmentation co-ordinates defined by the mass and charge-asymmetry coordinates as

$$\eta_A = \frac{A_1 - A_2}{A}; \quad \eta_Z = \frac{Z_1 - Z_2}{Z} \quad (2.10)$$

Here $A = A_1 + A_2$, $Z = Z_1 + Z_2$ and $N = N_1 + N_2$, A_i , Z_i and N_i ($i = 1; 2$) are respectively, the mass number, the charge number and the neutron number of two fragments. A , Z and N are respectively the mass number, charge number and neutron number of the compound system. The

limiting values of η are $0 < \eta < 1$, and thus allows a unified description of a few-nucleon or multi-nucleon (a cluster) transfer, a large-mass transfer, the complete fusion ($\eta = 1$) of nuclei and the symmetric ($\eta = 0$), asymmetric and super-asymmetric fission of a nucleus or compound nucleus.

The η_z coordinate gives the associated charge distribution effects.

(iii) The deformation co-ordinates $\beta_{\lambda i}$ ($\lambda, = 2, 3, 4 \dots$ and $i = 1, 2$) of the colliding nuclei or fragments.

(iv) The orientation degrees of freedom θ_i ($i = 1, 2$) of the deformed nuclei.

(v) Azimuthal angle Φ between the principal planes of the two colliding nuclei.

(vi) Neck length parameter.

2.3 Preformation probability (P_0):

Once the Hamiltonian is established, the Schrödinger equation in mass fragmentation co-ordinate η can be solved. On solving numerically, $|\psi^v(\eta)|^2$ gives the probability P_0 of finding the mass fragmentation η at a fixed R on the decay path.

$$P_0(A_2) = |\psi^v(A_2)|^2 \quad (2.11)$$

For fission studies, like the spontaneous fission and fission through the barrier, the motion in R at the saddle point is adiabatically slow as compared to the η motion. Therefore, the potential is minimized in the neck and deformation coordinates β_1 and β_2 at each R and η values. Starting from the nuclear ground state in spontaneous fission or cluster decay, and to have complete adiabaticity, only the lowest vibrational state $\nu = 0$ is occupied. Then, the mass (or charge) distribution yield, proportional to the probability $|\psi^{(0)}(\eta)|^2$ or $|\psi^{(0)}(\eta_z)|^2$ of finding a certain

mass (or charge) fragmentation η (or ηZ) at a position R on the decay path, when scaled to, say, mass A_2 of one of the fragments ($d\eta = 2/A$) is given by:

$$Y(A_2) = \left| \psi_R^{(0)}(A_2) \right|^2 \frac{2}{A} \sqrt{B_{\eta\eta}(A_2)}. \quad (2.12)$$

However, if the system is excited or we allow interaction between various degrees of freedom, higher values of ν would also contribute. These enter via the excitation of higher vibrational states, and through the temperature dependent potential V and masses B_{ij} . The effect of adding temperature on potential V and masses B_{ij} is to reduce the shell effects in them, resulting finally in the liquid drop potential VLDM and smoothed (averaged) masses B_{ij} for the systems to be very hot. Apparently, cold fission means taking both the potential V and masses B_{ij} with full shell effects included in them and hot fission means using the VLDM and smoothed (averaged) masses B_{ij} . Note that we are dealing here with a directly measurable quantity. The mass (or charge) asymmetry, which works dynamically as mass (or charge) transfer coordinate. Thus, the calculated yields $Y(A_i)$ (or $Y(Z_i)$) are directly comparable with experiments. The nuclear shape, once minimized in the neck and deformation coordinates β_1 and β_2 at a given R ($=R_{\text{saddle}}$), remains fixed for both the mass and charge distributions of fission or decay fragments.

2.4 Penetration Probability P:

Penetrability P measures the capability of fragments nucleus to penetrate the potential barrier generalized during compound nucleus formation.

The penetrability P in equation (2.2) is the WKB integral between R_a and R_b .

$$P = \exp\left[-\frac{2}{h} \int_{R_a}^{R_b} \{2\mu[V(R) - Q_{\text{eff}}]\}^{\frac{1}{2}} dR\right] \quad (2.13)$$

Solved analytically [9] with R_b as the second turning point.

Reference:

- [1] R. Kumar & M. K. Sharma Phys. Rev. C 85, 054612 (2012) ; D. Jain, R. Kumar, M. K. Sharma & R.K Gupta, Phys. Rev. C 85, 024615 (2012).
- [2] M. K. Sharma, G. Sawhney, R. K. Gupta, W. Grenier, J.Phys.G:Nucl.Part.Phys. 38 105101 (13pp) (2011); K. Sandhu, M. K. Sharma, R. K. Gupta, Phys. Rev. C 85 024604 (2012).
- [3] B. B. Singh. M. K. Sharma and R. K. Gupta, Phys. Rev. C 77 054613 (2008); M. Kaur, R. Kumar and M. K. Sharma Phys. Rev. C 85 014609 (2012); M. Kaur, M. K. Sharma Phys. Rev. C 85 054605 (2012).
- [4] R. K. Gupta, M. Balasubramaniam, R. Kumar, N. Singh, M. Manhas, and W. Greiner, J. Phys. G: Nucl. Part. Phys. C 31, 631 (2005); M. Manhas and R. K. Gupta, Phys. Rev. C 72, 024606 (2005).
- [5] R. K. Gupta, M. Manhas, G. MÄunzenberg, and W.Greiner, Phys. Rev. C 72, 014607.
- [6] J. Maruhn and W. Grenier, Z. Phys. 251, 431 (1972).
- [7] R. K. Gupta and W. Grenier, in Heavy Elements and Related New Phenomena, edited by W. Grenier and R. K. Gupta, Vol. I (World Scientific, Singapore 1999).
- [8] R. K. Gupta, M. K. Sharma, S. Singh, R. Nouicer and C. Beck, Phys. Rev. C 56, 3242 (1997); R. K. Gupta, M. K. Sharma, N. V. Antonenko and W. Scheid, J. Phys. G: Nucl. Part. Phys. 25, L47 (1997); M. K. Sharma, R. K. Gupta, and W. Scheid, *ibid.* 26, L45 (2000).
- [9] S.S Malik and R. K. Gupta, Phys. Rev. C. 39, 1992 (1989).

Chapter 3

Calculation and result:

Experimental challenges to produce super-heavy nuclei have been achieved by using heavy ion fusion reaction. The complex process of fusion of two heavy nuclei can be best understood via the decay products of compound nucleus (CN), such as the fusion evaporation residue (ER), the fusion-fission process along in the competing non-compound nucleus processes like quasi-fission and deep inelastic collision (DIC).

In this work, the **Dynamical cluster decay model** (DCM) [1-5] has been applied to study the Fission dynamics of ^{268}Sg nucleus formed in $^{30}\text{Si}+^{238}\text{U}$ reaction. It may be noted that DCM has been applied quite extensively for understanding the decay mechanism of compound system formed in heavy ion reactions. It has been applied for a large number of heavy ion reactions in length, intermediate, heavy and heavy and super-heavy mass region.

The fission cross-sections for the decay of ^{268}Sg have been observed over a wide range of centre of mass energy $E_{\text{cm}} = (124-169.5)$ MeV [6]. The level density parameter used here for calculations is $a=A/9$. The calculations are done within DCM by fitting the neck length parameter (ΔR). To see the effect of deformations and orientations the calculation has been done by including deformation in minimum optimum orientation approach. It is relevant to mention here that the question of magic numbers above $Z=82$ & $N=126$ is still open. A large number of theoretical & experimental attempts have been tried in past and $N=184$ is almost established as super heavy neutron number but $Z=114$, 120 & 126 still complete for proton magic number is super heavy mass region. For present calculation we have taken $Z=126$ & $N=184$ respectively as proton & neutron shell closer in heavy & super heavy region for fragments with $Z>82$ & $N=126$.

TABLE 3.1 DCM based fission cross-section for decay of ^{268}Sg formed in $^{30}\text{Si}+^{238}\text{U}$ reaction at all energy considering quadrupole (β_2) deformations within optimum orientation [7].

S.NO.	E _{cm} (MeV)	E _{CN} (MeV)	Temp (MeV)	ΔR (fm)	l_{max}	Σ_{DCM} (mb)	Σ_{Exp} (mb)
1.	124.900	31.364	1.043	0.9163	121	0.129	0.129
2.	128.939	35.402	1.072	0.9430	125	3.14	3.11
3.	133.975	40.435	1.182	0.9720	127	20.2	20.62
4.	138.972	45.435	1.252	1.0045	130	66.8	66.66
5.	143.981	50.445	1.318	1.0274	132	151	155.17
6.	148.978	55.441	1.381	1.0512	133	270	270.15
7.	154.027	60.490	1.442	1.0654	134	396	399.9
8.	159.062	65.526	1.500	1.0870	136	620	621.74
9.	169.18	75.571	1.609	1.1890	139	718	788.50

Table 3.1 shows the fission cross-section of $^{30}\text{Si}+^{238}\text{U} \rightarrow ^{268}\text{Sg} \rightarrow A_1+A_2$ reaction calculated using DCM compared with the experimental data. One can clearly see that DCM based calculations find nice comparison with the experimental data. Within DCM, the calculation are done by fitting the only parameter of the model known as neck length parameter “ ΔR ” shown in table 1 and depicted later in Fig 3.7.

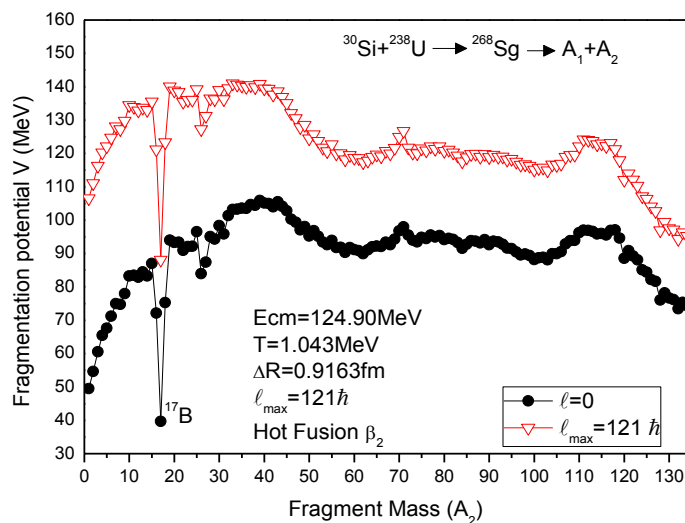


Fig 3.1 (a) shows the fragmentation potential as the function of fragment mass considering β_2 deformed fragmentation path at lowest energy $E_{cm}=124.90$ MeV.

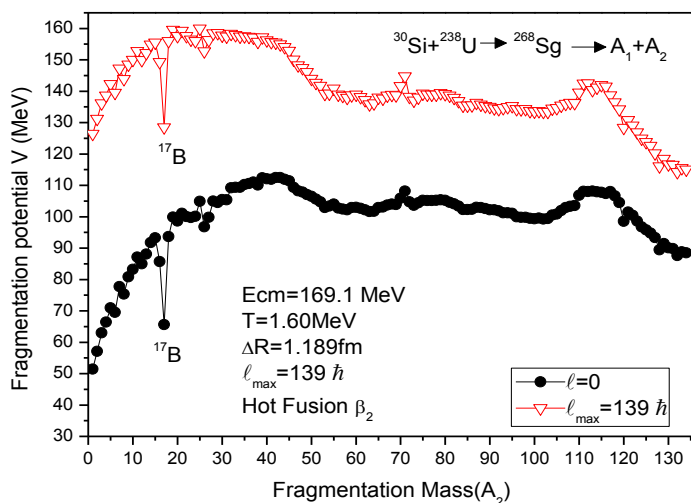


Fig 3.1 (b) shows the fragmentation potential as the function of fragment mass considering β_2 deformed fragmentation path energy at highest $E_{cm}=169.1$ MeV.

Fig 3.1 shows the fragmentation potential for ^{268}Sg nucleus at extreme value of angular momentum i.e $l=0$ and $l=l_{max}$ at (a) lowest energy (b) highest energy. It is clear from Fig 3.1 that

at $l=0$, ER are dominating. However, at $l=l_{max}$ fission fragments start contributing. Fig 3.1 (a) and (b) clearly depicts that the potential energy surfaces are not changing much with the increase in energy as well as angular momentum. The fragmentation with mass number $A_2=16-18$ show dips in the PES which implies that they are preferred but because of negligibly small value of penetrability (as shown later in fig 3.3 & 3.4) they are not contributing much towards the fragmentation process.

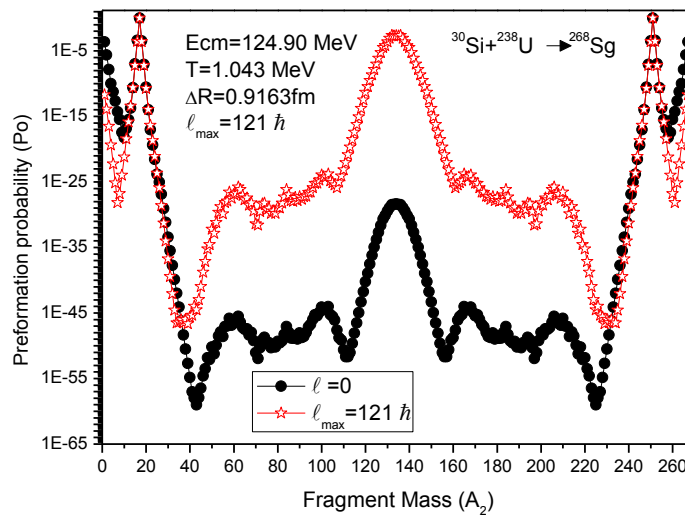


Fig 3.2 (a) shows the preformation probability as the function of fragment mass for ^{268}Sg compound system at lowest energy $E_{cm}=124.90$ MeV.

Fig 3.2(a) and 3.2(b) show the preformation probability for ^{268}Sg nucleus as a function of fragment mass number respectively at lowest energy $E_{cm}=124.90$ MeV and higher energy $E_{cm}=169.1$ MeV. It is important to note that the preformation probability is the probability of formation of fragment, which imparts important nuclear structure information and is a very useful quantity in the frame work of DCM.

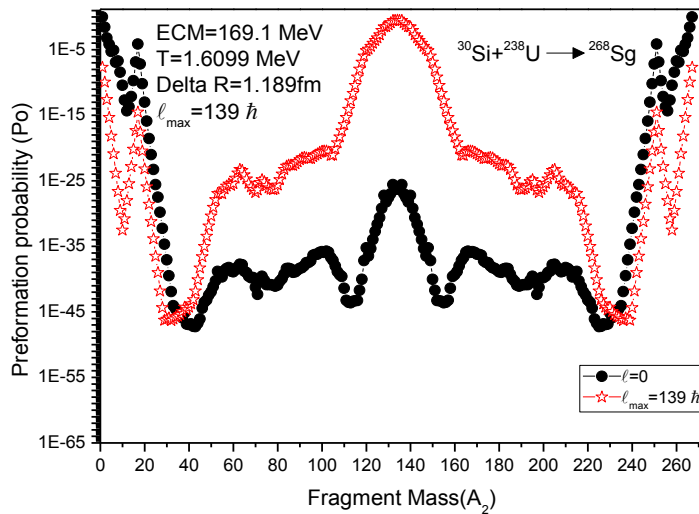


Fig 3.2 (b) shows the preformation probability as the function of fragment mass for deformed system at highest energy $E_{cm}=169.1$ MeV.

It can be seen from Fig 3.2 (a) & (b) that the mass distribution for the decay of ^{268}Sg is symmetric independent of energy of beam and remains the same at lower as well as higher l -values, with only difference that at lower l values the ER are dominating however at higher l -value fission fragments start contributing. Fig 3.2 further emphasize that the structure is not changing much with energy as well as angular momentum. Although preformation probability is relatively large at higher E_{cm} value for $l=0$ as well as for $l=l_{max}$ case.

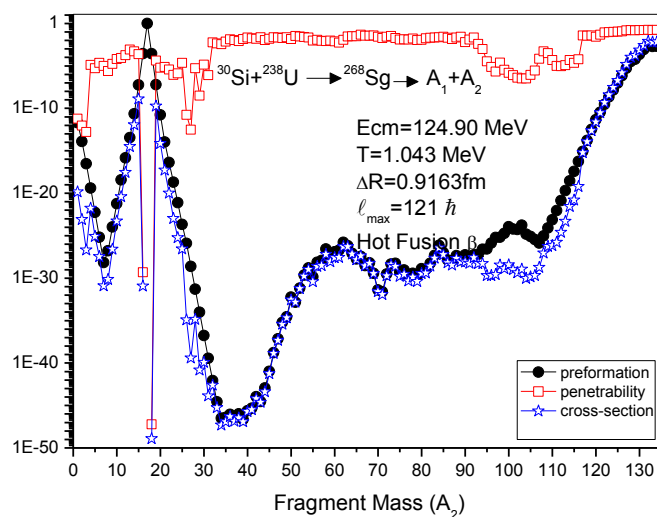


Fig 3.3 Preformation probability, Penetrability and cross-section as the function of mass fragments A_2 at $E_{cm}=124.90$ MeV.

Fig 3.3 shows the variation of penetrability, preformation probability, cross-section as the function of fragment mass at lowest energy $E_{cm}=124.90$ MeV. Fig 3.3 clearly depicts that cross-section follows the preformation probability behavior this observation emphasize the fact that preformation, probability imparts important nuclear structure information. The dips present at $A_2=16-18$ corresponds to the earlier closer value in Fig 3.1, which arise possibly due to inappropriate estimation of quadrupole deformation for these fragment. One may clearly see from Fig 3.3 that there is hardly any structure in the penetrability value and seem to contribute only towards the magnitude. Penetrability P measures the capacity of fragments nucleus to penetrate the potential barrier generalized during compound nucleus formation.

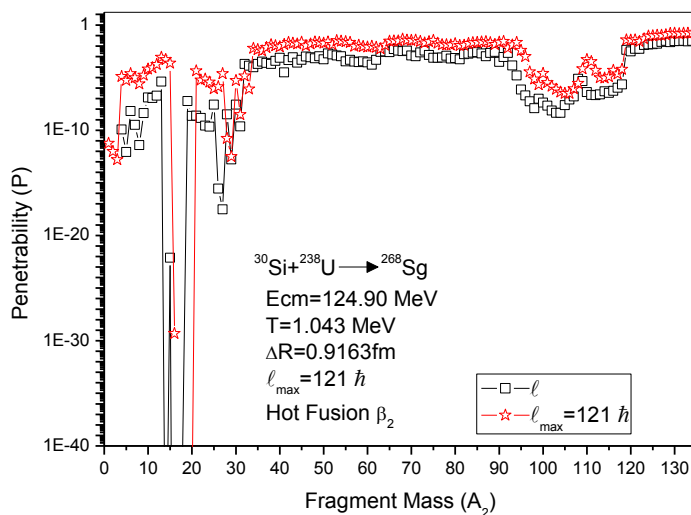


Fig: 3.4 (a) penetrability as a function of mass fragments A_2 at $E_{\text{cm}} = 124.90$ MeV.

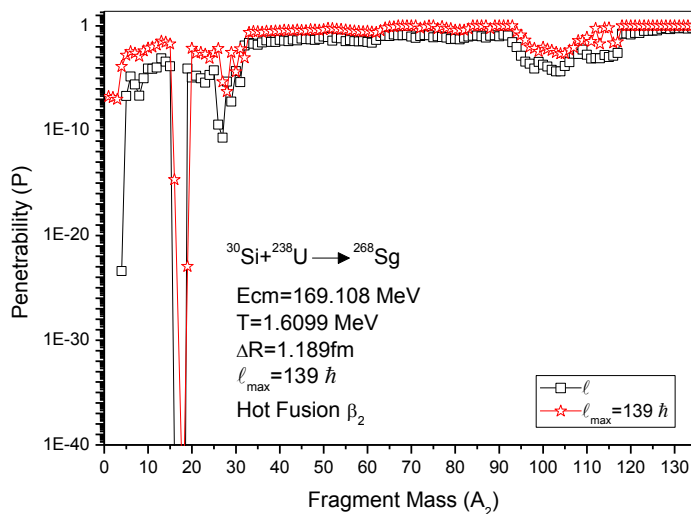


Fig: 3.4 (b) penetrability as a function of mass fragments A_2 at $E_{\text{cm}} = 169.108$ MeV.

Fig 3.4 (a) & 3.4 (b) show the variation of penetrability P with fragment mass A_2 for reaction $^{30}\text{Si} + ^{238}\text{U}$ respectively at $E_{\text{cm}} = 124.90$ MeV & $E_{\text{cm}} = 169.1$ MeV. Here again one may see the penetrability contributes mostly towards magnitudes, except for some structure in mass range

$A_2= 85-120$. The large dips in mass range $A_2=14-18$ may be ignored as they get counter balanced by the dips noted in Fig 3.1.

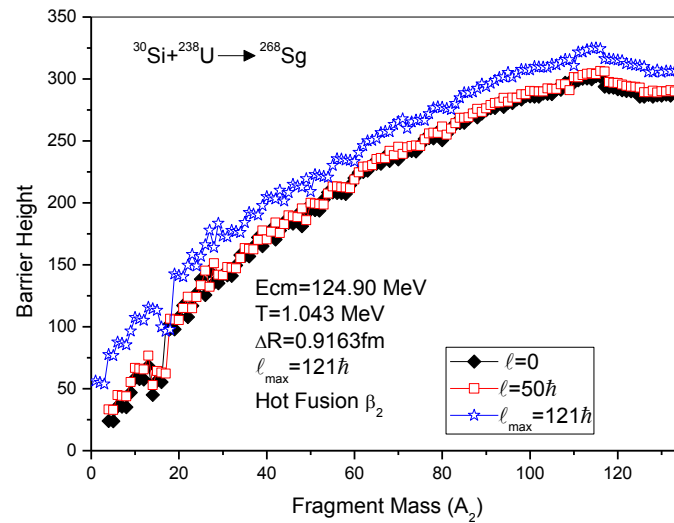


Fig: 3.5 Decay of barrier height as a function of mass fragments A_2 at lowest energy

$E_{cm}=124.90$ MeV.

It is clear from Fig 3.5 that decay barrier height increases as a function of fragment mass and it is independent of the angular momentum. This observation is similar to the one observed for heavy mass nuclei ^{204}Po and ^{215}Fr nuclei [8, 9].

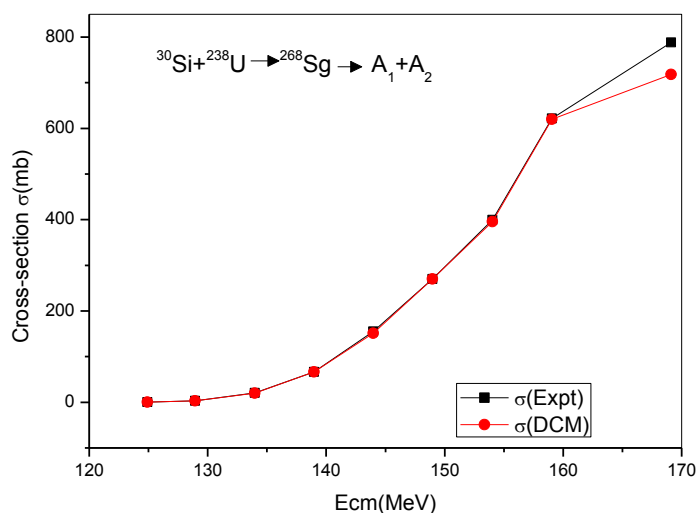


Fig: 3.6 DCM based cross-section compared with experiment.

Fig 3.6 shows the cross-section as a function of energy E_{cm} . It is clear from fig 3.4 and table 1 that the DCM calculated cross-section is in nice agreement with the experimental values except at one highest energy. This difference between calculated & measured cross-section may be associated with some non compound nucleus contribution at the highest energy. This quasi fission (NCN component) is estimated within DCM by taking $P_0=1$ and assuming that the entrance channel is not losing its identity i.e. the exit channel is the same as that of the entrance channel. The observed difference of 70 mb was fitted by taking neck length parameter $\Delta R= 1.34$ fm. This value of ΔR is higher than the one taken for fitting the fission data at this energy. Which mean to indicate that quasi fission process occurs relatively at earlier stage as compared to the fission?

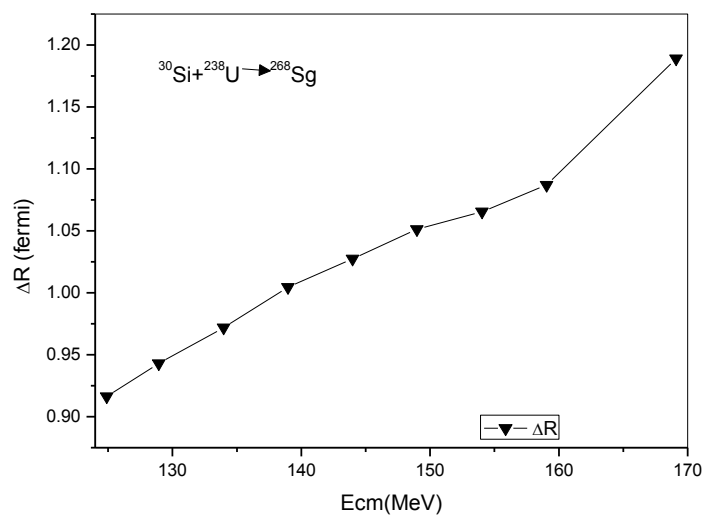


Fig 3.7 Neck length parameter as a function of Ecm

Fig 3.7 gives variation of ΔR with Ecm. It is observed that the neck length parameter increases almost linearly as a function of Ecm for $^{30}\text{Si} + ^{238}\text{U}$ reaction. It is relevant to mention here that ΔR is the only parameter of model and plays an important role in deciding decay path of nuclear system formed in heavy ion reactions.

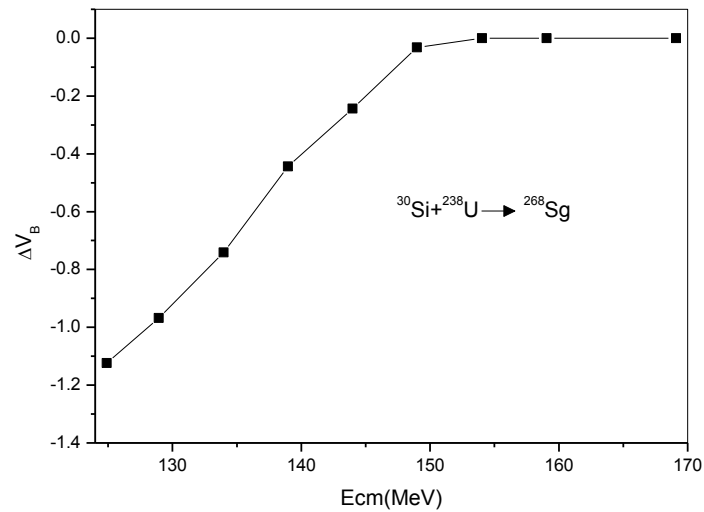


Fig: 3.8 ΔV_b as a function of Ecm.

Because of the inclusion of neck length parameter ΔR in DCM, the barrier modification $\Delta V_B = (V_B - V_{Ra})$ gets introduced automatically in the calculation. Hence V_B is the maximum barrier height & V_{Ra} is the barrier penetration height. This barrier modification is of great significance to handle the phenomena related to fusion hindrance at below barrier energies, as signified by the coupled channel calculation [10]. Fig 3.8 depicts the variation of ΔV_B as a function of Ecm. One can see that at higher Ecm values above 150 MeV barrier modification is almost negligible, whereas at near & below barrier energies significant barrier modification is observed for $^{30}\text{Si} + ^{238}\text{U}$ reaction.

SUMMARY

In summary, the fusion fission dynamics of $^{30}\text{Si}+^{238}\text{U}$ is investigated in context of DCM by including quadrupole deformation effects, level density parameter $A/9$ and super heavy magics as $Z=126$ & $N=184$. The observed fusion-fission data spread around the coulomb barrier has been fitted nicely using DCM based calculation, excepts for one higher energy, $E_{cm} = 169.10$ MeV. At this energy some 10 % contribution of quasi fission is predicted. The fragmentation path of ^{268}Sg formed in $^{30}\text{Si}+^{238}\text{U}$ reaction do not depend much on angular momentum & energy of incident beam. The fission distribution is clearly symmetric independent of l and E_{cm} values and barrier modification seems to be operating at near & below barrier energies.

It could be of further interest to investigate this reaction by taking different proton magic shell closures like $Z=114$ & 120 . Beside of this the choice of higher multipole deformations may imparts further insite to the dynamics of this reaction.

Reference:

- [1] R. Kumar & M. K. Sharma Phys. Rev. C 85, 054612 (2012) ; D. Jain, R. Kumar, M. K. Sharma & R.K Gupta, Phys. Rev. C 85, 024615 (2012).
- [2] M. K. Sharma, G. Sawhney, R. K. Gupta, W. Grenier, J.Phys.G:Nucl.Part.Phys. 38 105101 (13pp) (2011); K. Sandhu, M. K. Sharma, R. K. Gupta, Phys. Rev. C 85 024604 (2012).
- [3] B. B. Singh. M. K. Sharma and R. K. Gupta, Phys. Rev. C 77 054613 (2008); M. Kaur, R. Kumar and M. K. Sharma Phys. Rev. C 85 014609 (2012); M. Kaur, M. K. Sharma Phys. Rev. C 85 054605 (2012).
- [4] R. K. Gupta, M. Balasubramaniam, R. Kumar, N. Singh, M. Manhas, and W. Greiner, J. Phys. G: Nucl. Part. Phys. C 31, 631 (2005); M. Manhas and R. K. Gupta, Phys. Rev. C 72, 024606 (2005).
- [5] R. K. Gupta, M. Manhas, G. M. Aunzenberg, and W. Greiner, Phys. Rev. C 72, 014607 (2005).
- [6] K. Nishio, H. Ikezoe, I. Nishinaka, S. Mitsuoka, K. Hirose, T. Ohtsuki, Y. Watanabe, Y. Aritomo, and S. Hofmann Phys. Rev. C **82**, 044604 (2010).
- [7] R. K. Gupta, M. Balasubramaniam, R. Kumar, N. Singh, M. Manhas, W. Grenier, J. P. G: Nucl. Part. Phys. 31, 631 (2005).
- [8] M. K. Sharma, G. Sawhney, R. K. Gupta, W. Grenier, J.Phys.G:Nucl.Part.Phys. 38 105101 (13pp) (2011); K. Sandhu, M. K. Sharma, R. K. Gupta, Phys. Rev. C 85 024604 (2012).
- [9] B. B. Singh. M. K. Sharma and R. K. Gupta, Phys. Rev. C 77 054613 (2008); M. Kaur, R. Kumar and M. K. Sharma Phys. Rev. C 85 014609 (2012); M. Kaur, M. K. Sharma Phys. Rev. C 85 054605 (2012).
- [10] Modified version of the CCFULL code, K. Hagino *et al.*, Comput. Phys. Commun. **123**, 143 (1999).